Effects of heterogeneity and prestress field on phonon properties of semiconductor nanofilms

Jiachuan Wang [a,b], Linli Zhu [a,b,*], Wenyan Yin [c,d]

[a] Department of Engineering Mechanics, Zhejiang University, Hangzhou 310027, China
[b] Key Laboratory of Soft Machines and Smart Devices of Zhejiang Province, Zhejiang University, Hangzhou 310027, China
[c] Innovative Institute of Electromagnetic Information and Electronic Integration, College of Information Science and Electronic Engineering, Zhejiang University, Hangzhou 310058, China
[d] Key Laboratory of Micro-Nano Electronics and Smart Systems of Zhejiang Province, Zhejiang University, Hangzhou 310058, China

ARTICLE INFO

ABSTRACT

The phonon dispersion relation, phonon group velocity and phonon density of state in GaN-based wurtzite nanofilms under prestress fields are investigated theoretically. Considering the acoustoelastic effects and spatial confinement effects, the acoustic phonons properties in stressed AlN/GaN/AlN nanofilms are derived by using the elasticity model, comparing with those in the pure AlN nanofilm and pure GaN nanofilm. Numerical simulations demonstrate that the heterogeneity in GaN-based nanofilms can modify the phonon dispersion relations of nanofilms, leading to the change of phonon group velocity and phonon density of state. The stress field can significantly affect the phonon properties of GaN-based heterostructural nanofilms, e.g. the positive stress decreases the phonon energy and group velocity while enhances the density of state. The influence of the stress field is also sensitive to the thickness of each component in heterostructural nanofilms. The present work will be useful in tuning the phonon properties through phonon engineering and strain/stress engineering to control the thermal and electrical performance in GaN-heterostructure-based electronic devices.

© 2017 Elsevier B.V. All rights reserved.

1. Introduction

With the increasing development in nanomechanical and nanoelectronic devices or systems, the semiconductor materials with low-dimensional structures like nanowires and nanofilms draw more and more attentions. When the dimensions are limited to nanometer level, semiconductor nanostructures could be extremely different with the bulk materials in physical and mechanical properties such as carrier mobility, electric resistance, thermal conductivity and elastic modulus. Due to the wide applications of semiconductor nanostructures in optoelectronics [1,2], resistive switching [3,4], and biochemical sensora [5,6], the optimization and modification for their properties have made great progress. Since the nanoelectronic devices or systems are facing difficulties in heat dissipation, it is critically necessary to give an insight into the thermal properties in nanostuctured semiconductors [7–11].

Phonons as the quanta of crystal vibration, especially acoustic phonons, are dominant in transporting heat in semiconductors. Because of that the thermal and electric properties of semiconductors are sensitive to the phonon properties, it is important to study phonon performance in nanostructured semiconductors which have been widely used in micro/nano electronic devices or systems [12–15]. For instance, Balandin and his coworkers [16] theoretically simulated the phonon propagation and dispersion relations in the GaN nanostructures covered with various materials such as AlN and plastic materials. Groenen [17] made the calculations for phonon dispersion relations in Si membranes and silicon-on-insulator structures. Zou and Balandin [18] discussed the decrease of thermal conductivity under phonon confinement and boundary scattering in a silicon nanowire.

To optimize the physics properties of semiconductor materials in micro/nano devices or systems, many efforts have been carried out to investigate the properties of hetero- and nanostructured semiconductors [19–22]. For example, Royo et al. [23] reviewed the growth, properties and applications of core-multishell semiconductor nanowires. Ajay et al. [24] made experiments to study the physical properties in planar and nanowires of Ge- and Si-doped GaN/AlN heterostructures, showing great electrical and optical performance. On the other hand, one can tune the ability of material based on the strain/stress engineering and surface/interface engineering through controlling multi-field coupling effects [25–30]. Luo and Zhu [31] calculated the phonon properties

---

of GaN nanofilms under surface stress and achieved the thermal conductivity variation in GaN nanofilms subjected to the surface stress. Li et al. [32] analyzed the stress/strain effects on the thermal management of nanostructured semiconductors including SWCNT and single-layer graphene. Zhu and Luo [33] simulated the thermal properties of GaN nanofilms through analyzing acoustic phonon properties under various stress fields. Shchepetov et al. [34] proposed a method to avoid buckling of released membranes by adding a strain compensating frame on ultra-thin suspended single crystalline flat silicon. However, there exist no researches how the prestress fields affect the phonon properties of nanostructured semiconductors with heterostructures.

In this work, we perform theoretical studies on the phonon properties of wurtzite (AlN/GaN/AlN) nanofilms under prestress fields. The homogeneous nanofilms with pure AlN or GaN nanofilms are also addressed for a comparison on phonon performance. The elastic model is applied to calculate the phonon dispersion relation of various structures under prestress fields, in which the acoustoelastic effects and spatial confinement effects are considered. Numerical results demonstrate that the heterogeneity can change the phonon properties in GaN-based nanofilms significantly, including the phonon dispersion relation, phonon group velocity and phonon state density. In addition, the prestress field can modify the phonon properties of the wurtzite AlN/GaN/AlN nanofilms. The theoretical model used for calculating phonon dispersion relation is presented in Section 2. The derivation for the phonon group velocity and density of state is presented in Section 3. After that, we display the outcomes of simulations in Section 4, and then draw our conclusions in Section 5.

2. Theoretical model

2.1. Confined phonons in heterostructured nanofilms

To analyze the acoustic phonon properties of heterostructures with spatial confinement effect, the continuum elasticity model which has been proved to describe the confined phonons successfully [35–40], is adopted to characterize the phonon properties in nanostructured semiconductors. The features in phonon modes of confined nanostructures could be derived with acoustic phonons of free-standing nanofilms. Let's begin with the vibration equations for an elastic solid as

$$\rho \frac{\partial^2 u_i}{\partial t^2} = \frac{\partial}{\partial x_j}\left(C_{ijkl}\frac{\partial u_k}{\partial x_l}\right), \tag{1}$$

where the displacement vector is defined as u_i, the three Cartesian coordinate axes are indicated with $i, j = 1, 2, 3$. ρ is, and C_{ijkl} is the four-order modulus tensor which is varied along the thickness in nanofilms with the presence of heterogeneity. There are only two independent elastic constants stated as C_{11} and C_{44} for isotropic materials when we contract the indices using the general rules: $(iijj) \rightarrow (ij)$ and $(12) \rightarrow (6)$, $(13) \rightarrow (5)$, $(23) \rightarrow (4)$. The x_3 direction is defined as the transverse direction of the thickness, as well as the hexagonal axis of the AlN and GaN crystal orientations in nano-

films. The in-plane directions are defined as x_1 and x_2. Thereby, the displacements of the nanofilm are the functions of x_1 and x_2, and the elastic modulus $C_{ij}(x_3)$ is the function of x_3. Then, we can write the displacement of Eq. (1) in the form of

$$u = \bar{u}(x_3)\exp[i(\omega t - k \cdot x_1)], \tag{2}$$

where ω is the frequency and k is the wave vector. $\bar{u}(x_3)$ is defined as the amplitude of displacement vector and i is imaginary unit. Using the solution of Eq. (2) to substitute the variables in the Eq. (1), the corresponding eigenvalue equation can be derived as

$$Ð\bar{u}(x_3) = -\rho\omega^2\bar{u}(x_3), \tag{3}$$

where

$$Ð = \begin{bmatrix} C_{44}\frac{d^2}{dx_3^2} - C_{11}k^2 + \frac{dC_{44}}{dx_3}\frac{d}{dx_3} & 0 & -ik(C_{13}+C_{44})\frac{d}{dx_3} - ik\frac{dC_{44}}{dx_3} \\ 0 & C_{44}\frac{d^2}{dx_3^2} - C_{66}k^2 + \frac{dC_{44}}{dx_3}\frac{d}{dx_3} & 0 \\ -ik(C_{13}+C_{44})\frac{d}{dx_3} - ik\frac{dC_{13}}{dx_3} & 0 & C_{33}\frac{d^2}{dx_3^2} - C_{44}k^2 + \frac{dC_{33}}{dx_3}\frac{d}{dx_3} \end{bmatrix} \tag{4}$$

We have already known that the boundary conditions are

$$\sigma_{13} = \sigma_{23} = \sigma_{33} = 0 \text{ at } x_1 = \pm a \tag{5}$$

Here, $2a$ is the thickness of nanofilms. For the shear modes (SH), the nanofilm has its displacement $\bar{u} = (0, \bar{u}_2, 0)$, leading to the dispersion relation from the eigenvalue equation as

$$C_{44}\frac{d^2\bar{u}_2}{dx_3^2} + (\rho\omega^2 - C_{66}k^2)\bar{u}_2 + \frac{dC_{44}}{dx_3}\frac{d\bar{u}_2}{dx_3} = 0 \tag{6}$$

For the dilatational modes (SA) and the flexural modes (AS), we can get the solution by using the symmetrical and anti-symmetrical properties for the Eq. (1) of u_1 and u_3. The corresponding eigenvalue equations are expressed as

$$C_{44}\frac{d^2\bar{u}_1}{dx_3^2} + (\rho\omega^2 - C_{11}k^2)\bar{u}_1 + \frac{dC_{44}}{dx_3}\frac{d\bar{u}_1}{dx_3} - ik(C_{13}+C_{44})\frac{d\bar{u}_3}{dx_3}$$
$$- ik\frac{dC_{44}}{dx_3}\bar{u}_3 = 0 \tag{7a}$$

$$C_{33}\frac{d^2\bar{u}_3}{dx_3^2} + (\rho\omega^2 - C_{44}k^2)\bar{u}_3 + \frac{dC_{33}}{dx_3}\frac{d\bar{u}_3}{dx_3} - ik(C_{13}+C_{44})\frac{d\bar{u}_1}{dx_3}$$
$$- ik\frac{dC_{13}}{dx_3}\bar{u}_1 = 0 \tag{7b}$$

With corresponding boundary conditions and different elastic modulus in GaN layer and AlN layer, the dispersion relations of SH, SA, AS modes can be solved numerically. In heterogeneous nanostructures, the interfaces could play a significant role in physical and mechanical performance. For convenience, it is supposed that the GaN layer and AlN layer are connected perfectly and the interface stress induced by lattice mismatch is neglected. During simulations, the displacement compatibility condition is applied in the interfaces between GaN layer and AlN layer.

Table 1
Material parameters of AlN/GaN/AlN nanofilm for calculations.

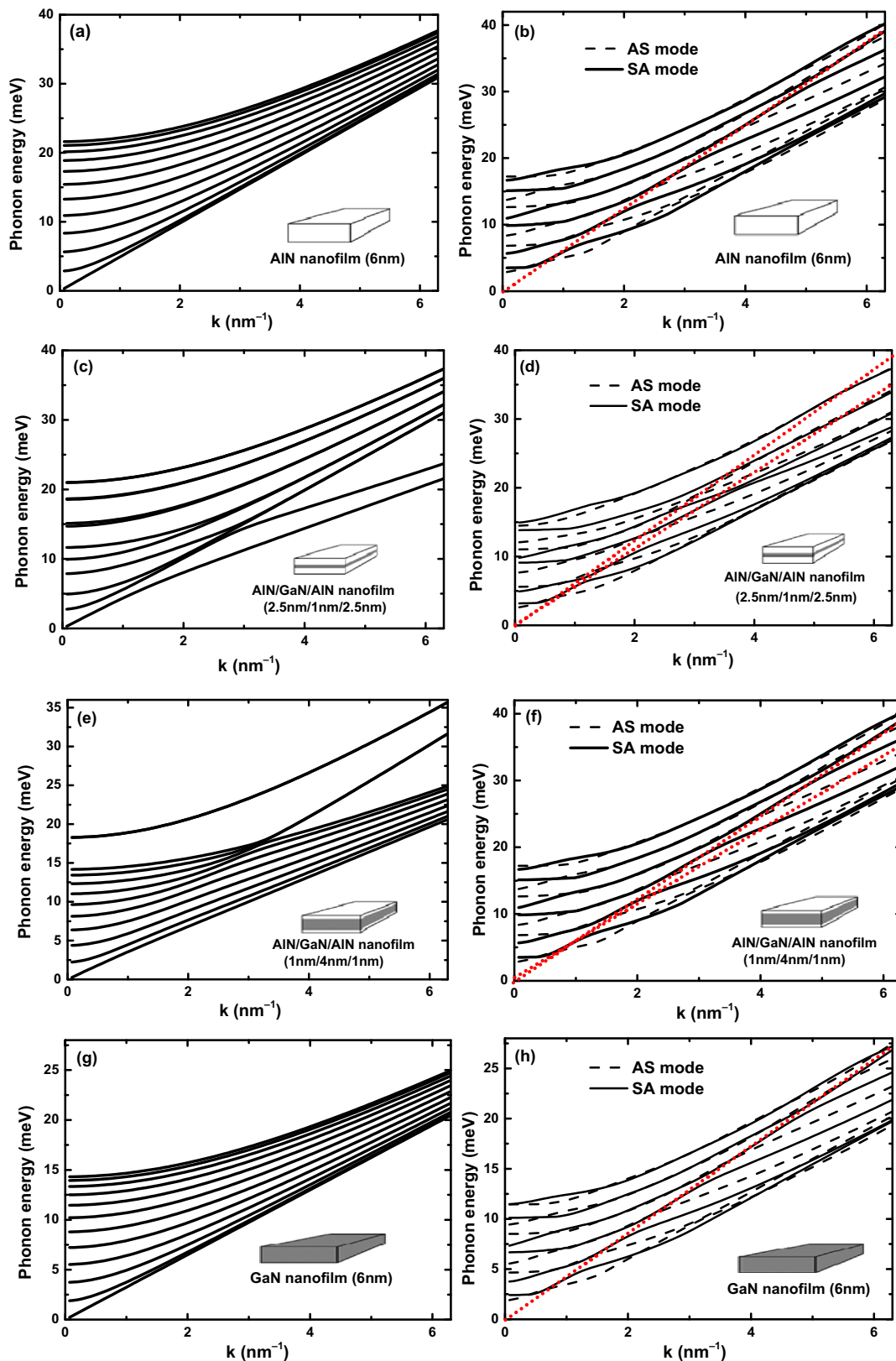| GaN	$C_{11}(GPa)$	$C_{13}(GPa)$	$C_{55}(GPa)$	$C_{111}(GPa)$	$C_{123}(GPa)$
	252	129	148	−1213	−253
	$C_{144}(GPa)$	$C_{155}(GPa)$	$C_{112}(GPa)$	$C_{456}(GPa)$	$\rho(kg/m^3)$
	−46	−606	−867	−49	6100
AlN	$C_{11}(GPa)$	$C_{13}(GPa)$	$C_{55}(GPa)$	$C_{111}(GPa)$	$C_{123}(GPa)$
	282	149	179	−1073	−61
	$C_{144}(GPa)$	$C_{155}(GPa)$	$C_{112}(GPa)$	$C_{456}(GPa)$	$\rho(kg/m^3)$
	57	−757	−965	−9	3235

Fig. 1. Phonon dispersion relations of the SH modes (a, c, e, g) and SA/AS modes (b, d, f, h). There are four types of nanofilms shown as pure AlN with 6 nm thickness for (a) and (b), AlN/GaN/AlN with 2.5 nm/1nm/2.5 nm width for (c) and (d), AlN/GaN/AlN with 1 nm/4nm/1nm width for (e) and (f), and pure GaN with 6 nm thickness for (g) and (h).
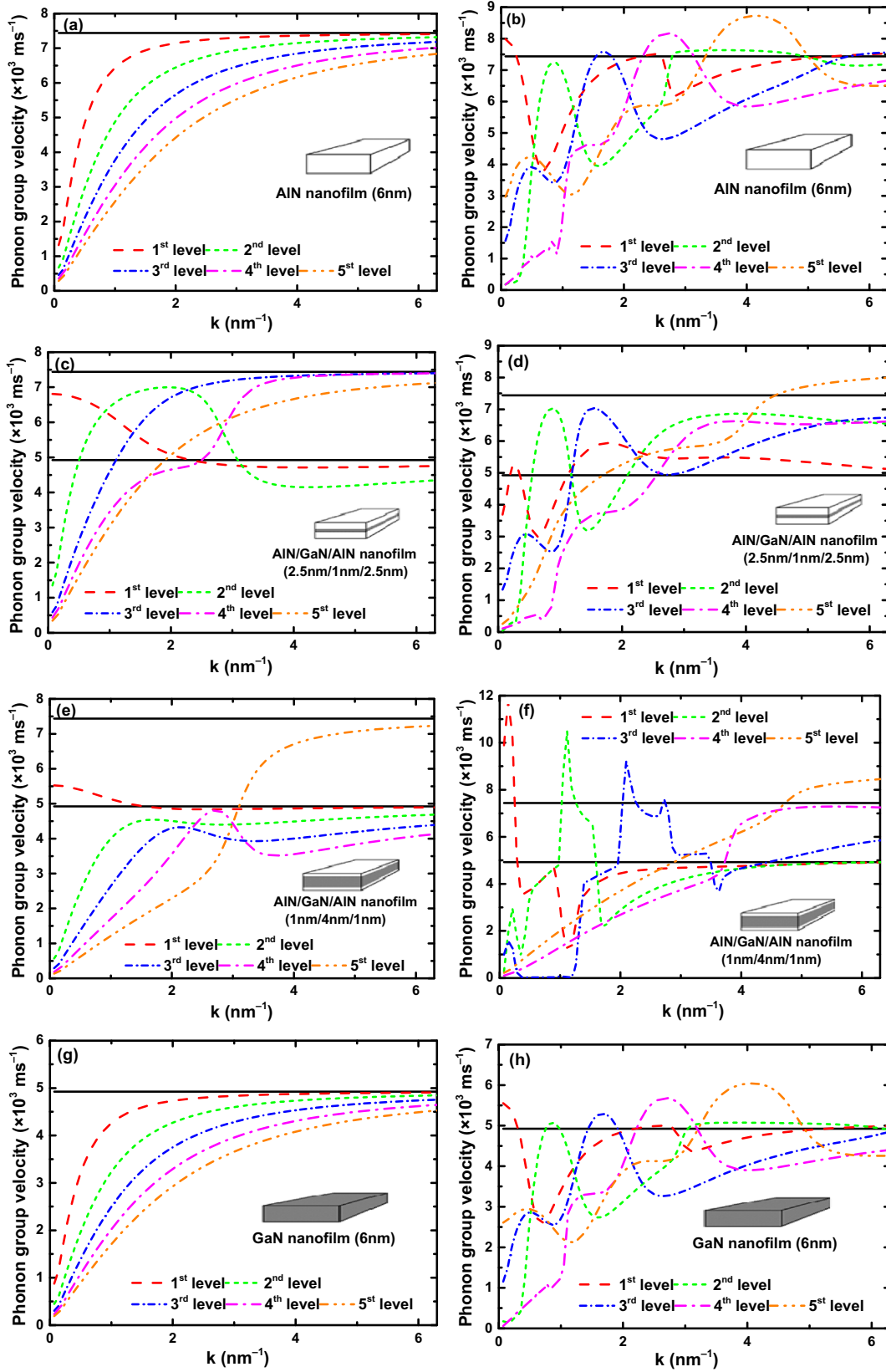
Fig. 2. Phonon group velocities of the SH (a, c, e, g) and SA modes (b, d, f, h). All four types of structures are calculated as AlN nanofilm (a, b), AlN/GaN/AlN with 2.5 nm/1nm/2.5 nm width (c, d), AlN/GaN/AlN with 1 nm/4nm/1nm width (e, f), and GaN nanofilm (g, h).
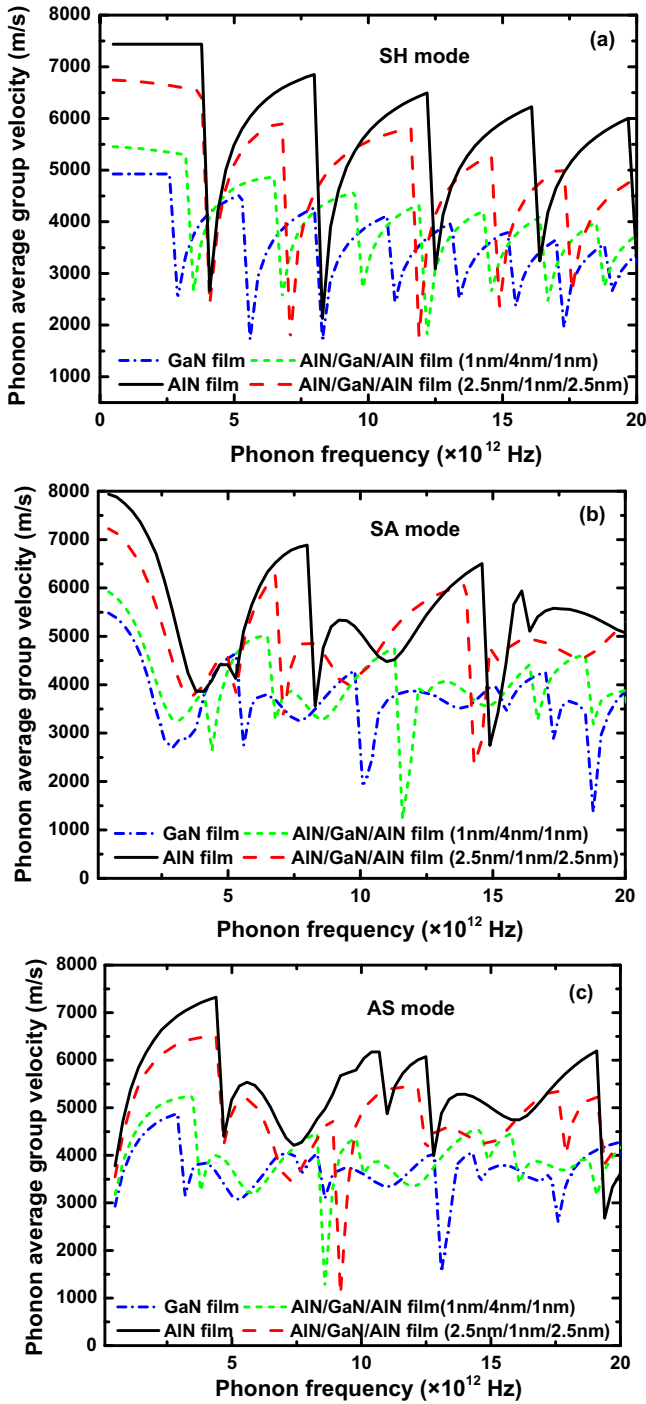
Fig. 3. Phonon average group velocities varied with phonon frequency for SH (a), SA (b), and AS (c) modes with four types of structures in nanofilms.
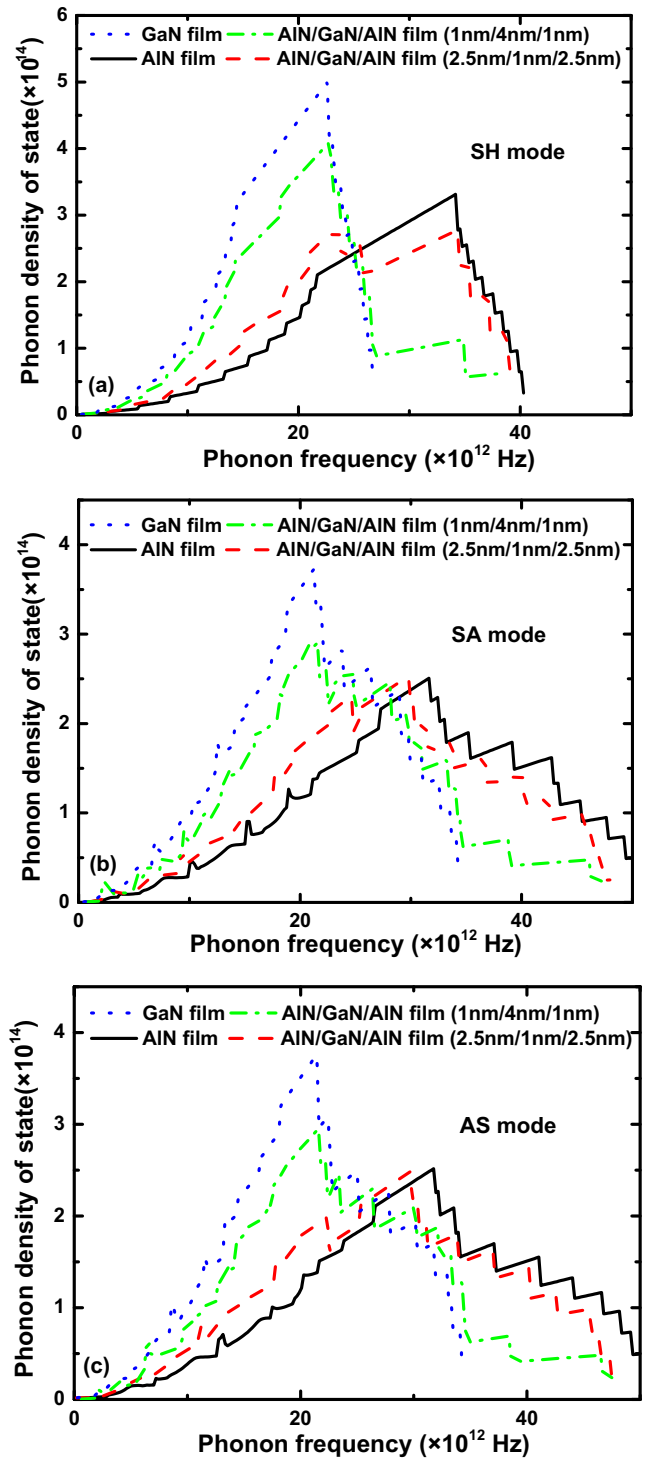

Fig. 4. Phonon density of states varied with phonon frequency for SH (a), SA (b), and AS (c) modes with various structures of nanofilms.

2.2. Acoustoelastic effects in nanofilms

When the semiconductor nanostructures are subjected to pre-stress fields, the phonon properties will be affected by the stress fields. It is well known that the vibration behaviors in stressed structures called as the acoustoelastic effects can be described in the framework of elastic theory [41,42]. Therefore, the acoustelastic theory is utilized to make a continuum description of the phonon properties in stressed nanofilms [13,33,43,44]. Suppose that nanofilms are acted by biaxially lateral stress that is equal in the two directions. As the isotropic material, the nanofilm has the initial stresses written as

$$\tilde{\sigma}_{11} = \tilde{\sigma}_{22} = \tilde{\sigma}_{33} = \sigma_0 \tag{8}$$

where the $\tilde{\sigma}_{ij}$ is defined as the initial stress (prestress) tensor. The variable with a subscript as 1 or 2 denotes the in-plane direction, whereas a subscript 3 denotes the transverse direction. Therefore, based on the constitutive relation of linear elasticity, we can derive the prestrain as
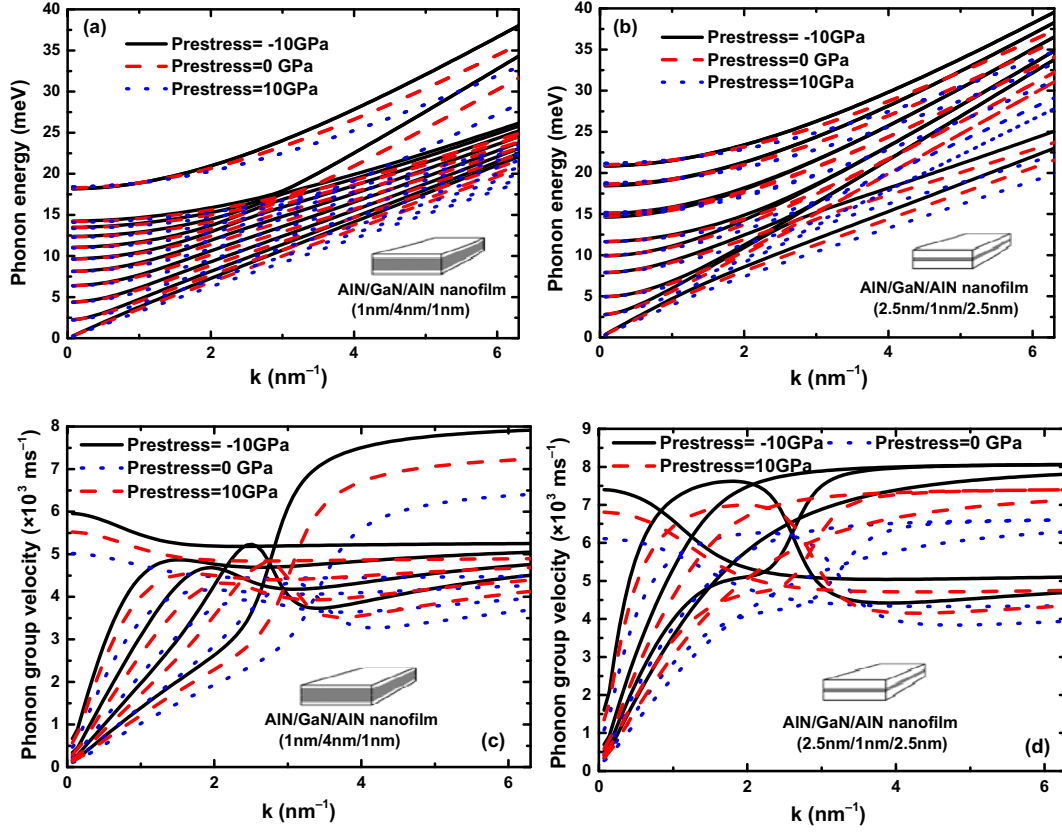
Fig. 5. Phonon energy (a, b) and phonon group velocities (c, d) varied with wave vector under various prestresses in heterostructural nanofilms AlN/GaN/AlN, with the 1 nm-4 nm-1 nm width (a, c) and 2.5 nm-1 nm-2.5 nm width (b, c) in SH modes as the examples.

$$u_{11}^0 = \frac{s_{22} - s_{12}}{s_{12}s_{22} - s_{12}^2}\sigma_0, \quad u_{22}^0 = \frac{s_{11} - s_{12}}{s_{11}s_{22} - s_{12}^2}\sigma_0,$$

$$u_{33}^0 = -\frac{C_{13}}{C_{33}}u_{11}^0 - \frac{C_{23}}{C_{33}}u_{22}^0, \tag{9}$$

where $s_{11} = C_{11} - C_{13}^2/C_{33}$, $s_{12} = C_{12} - C_{13}C_{23}/C_{33}$, and $s_{22} = C_{22} - C_{23}^2/C_{33}$. Due to the existence of biaxial stress, we can discover the acoustoelastic effects on the phonons in stressed nanostructures. So, the motion equation of elastic vibration can be modified as

$$\rho^N \frac{\partial^2 u_i}{\partial t^2} = \frac{\partial}{\partial x_j}\left(\hat{C}_{ijkl}\frac{\partial u_k}{\partial x_l}\right) + \sigma_0 \frac{\partial^2 u_i}{\partial x_1^2}, \tag{10}$$

in which density after deformation is defined as $\rho^N \approx \rho(1 - \Delta u^0)$ (where $\Delta u^0 = u_{11}^0 + u_{22}^0 + u_{33}^0$) and the modified effective elastic modulus tensor is denoted as $\hat{C}_{ijkl}$, given by

$$\hat{C}_{ijkl} = C_{ijkl}\left(1 + u_{ii}^0 + u_{jj}^0 + u_{kk}^0 - \Delta u^0\right) + C_{ijklmn}u_{mm}^0, \tag{11}$$

in which all the non-zero elements of the effective elastic modulus are expressed as

$$\hat{C}_{11} = C_{11}(1 + 2u_{11}^0 - u_{33}^0) + (C_{111} + C_{112})u_{11}^0 + C_{112}u_{33}^0$$

$$\hat{C}_{33} = C_{11}(1 + 2u_{11}^0 - u_{33}^0) + 2C_{112}u_{11}^0 + C_{111}u_{33}^0$$

$$\hat{C}_{44} = C_{44}(1 + 2u_{11}^0 - u_{33}^0) + (C_{144} + C_{155})u_{11}^0 + C_{155}u_{33}^0$$

$$\hat{C}_{12} = C_{12}(1 + u_{33}^0) + 2C_{112}u_{11}^0 + C_{123}u_{33}^0 b$$

$$\hat{C}_{13} = C_{12}(1 + u_{33}^0) + (C_{123} + C_{112})u_{11}^0 + C_{112}u_{33}^0 \tag{12}$$

where $\hat{C}_{22} = \hat{C}_{11}$, $\hat{C}_{23} = \hat{C}_{13}$, $\hat{C}_{55} = \hat{C}_{44}$, and $\hat{C}_{66} = (\hat{C}_{11} - \hat{C}_{22})/2$, C_{ijklmn} is the third-order elasticity tensor. The function of the wave vector and the frequency in the AS/SA modes and SH modes can be rewritten from the Eq. (10). For instance, in the SH modes the dispersion relation can be re-derived as

$$\rho^N\omega^2 = \hat{C}_{44}k_{x_3}^2 + (\hat{C}_{66} + \sigma_0)k^2. \tag{13}$$

Then we can get the relations of phonon dispersion for the stressed GaN layer and stressed AlN layer in SA/AS modes as well.

3. Phonon group velocity and density of state

Once we derive the phonon dispersion relations of a variety of modes for nanofilms, the phonon frequency varied with the phonon wave vector k can be calculated using the finite difference method. Therefore, the phonon group velocity could be derived by the numerical differentiation as following

$$v_n(k) = \frac{d\omega_n(k)}{dk} \tag{14}$$

Within a particular defined phonon n, the corresponding v_n and ω_n can be derived respectively. As the phonon is spatially confined caused by the boundaries along the cross-plane (x_1 and x_2) direction, the lattice wave that propagates along the z-axis is increasingly quantized, leading to the variation of phonon branches. Different from the group velocity which describes the velocity of the wave packet of every phonon branches respectively, the average group velocity is used to character the velocity of wave package with every mode populated for each polarization. According to Callaway's function, the average phonon group velocity depended on frequency could be written as [36]
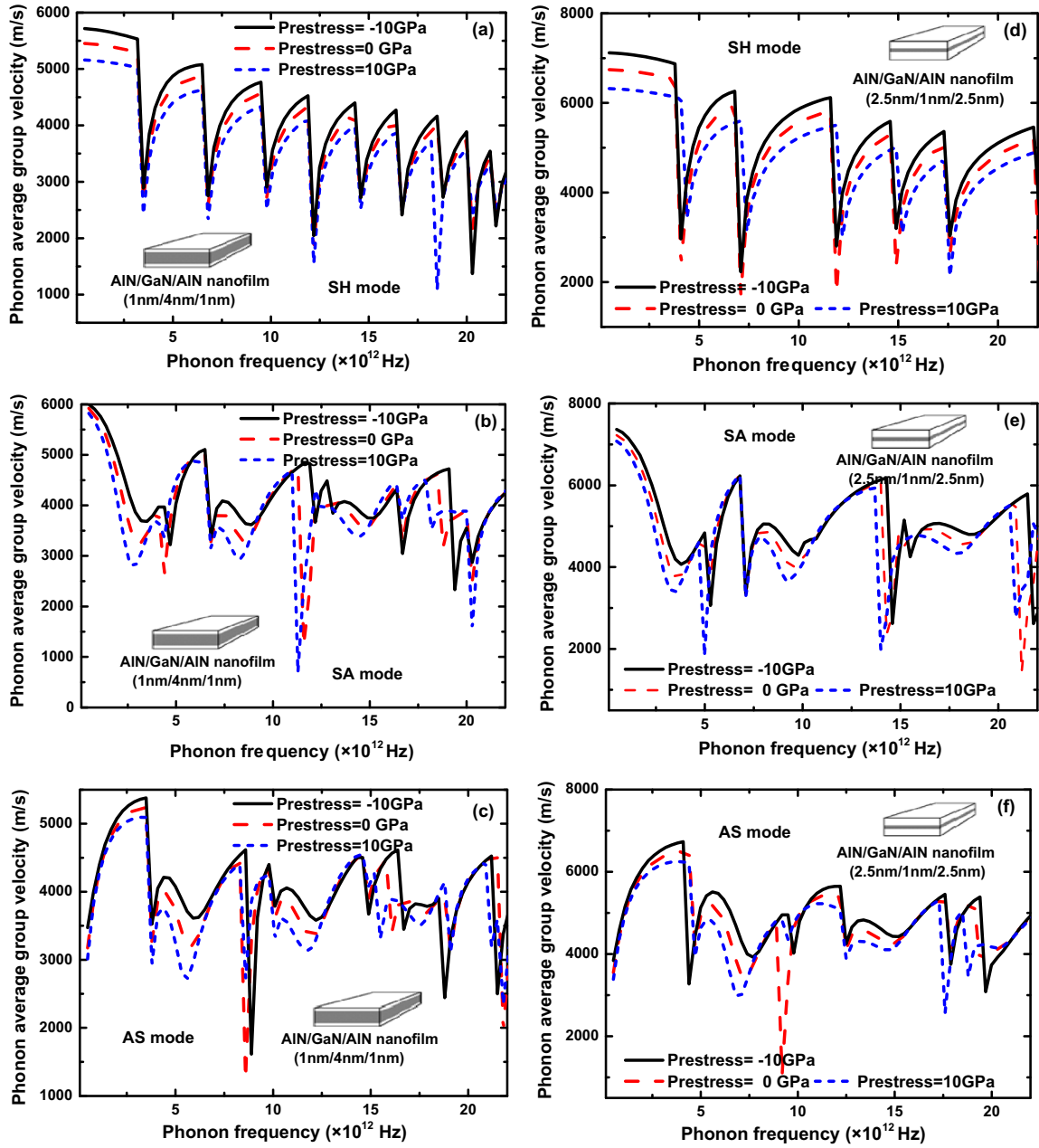
Fig. 6. Phonon average group velocities varied with the phonon energy for different modes and heterostructures under prestress fields. AlN/GaN/AlN nanofilms with 1 nm-4 nm-1 nm width (a–c) and 2.5 nm-1 nm-2.5 nm width (d–f).

$$\bar{V}(\omega) = \left\{ \frac{1}{m(\omega)} \sum_{n=1}^{m(\omega)} [V_n(\omega)]^{-1} \right\}^{-1}, \tag{15}$$

in which the average phonon group velocity is defined as $\bar{V}(\omega)$ and the number of phonon branches.

In order to analyze thermal properties of semiconductor nanostructures, the total amount of phonon modes per unit volume in the crystal of a unit frequency interval, called as phonon density of state (DOS), is required at a given phonon frequency. For the quasi-2D phonon DOS, one can combine the group velocity and confined phonon dispersion relations to obtain the DOS of nanofilms, given as

$$f_n^{SA,AS,SH}(\omega) = \frac{1}{H} \left[\frac{1}{2\pi} k_n^{SA,AS,SH}(\omega) \frac{1}{v_n^{SA,AS,SH}} \right], \tag{16}$$

in which the thickness of nanofilms is defined as H, the number of phonon branches is counted as n, and the phonon group velocity is v. The types of polarization SA, AS, SH are supposed to be calculated respectively with different superscript. Then one can get the total DOSs for all polarizations by summing up n phonon branches as $F(\omega) = \sum_n f_n(\omega)$.

4. Results and discussion

For the sake of discussing the phonon properties of GaN-based heterostructures under prestress qualitatively, the numerical results of phonon properties for three different nanofilms models are presented in this section. Here, the elastic modulus of GaN and AlN are displayed in Table 1 [45]. According to the theoretical description in Sections 2 and 3, we simulate the phonon properties including the phonon dispersion relation, phonon group velocity,
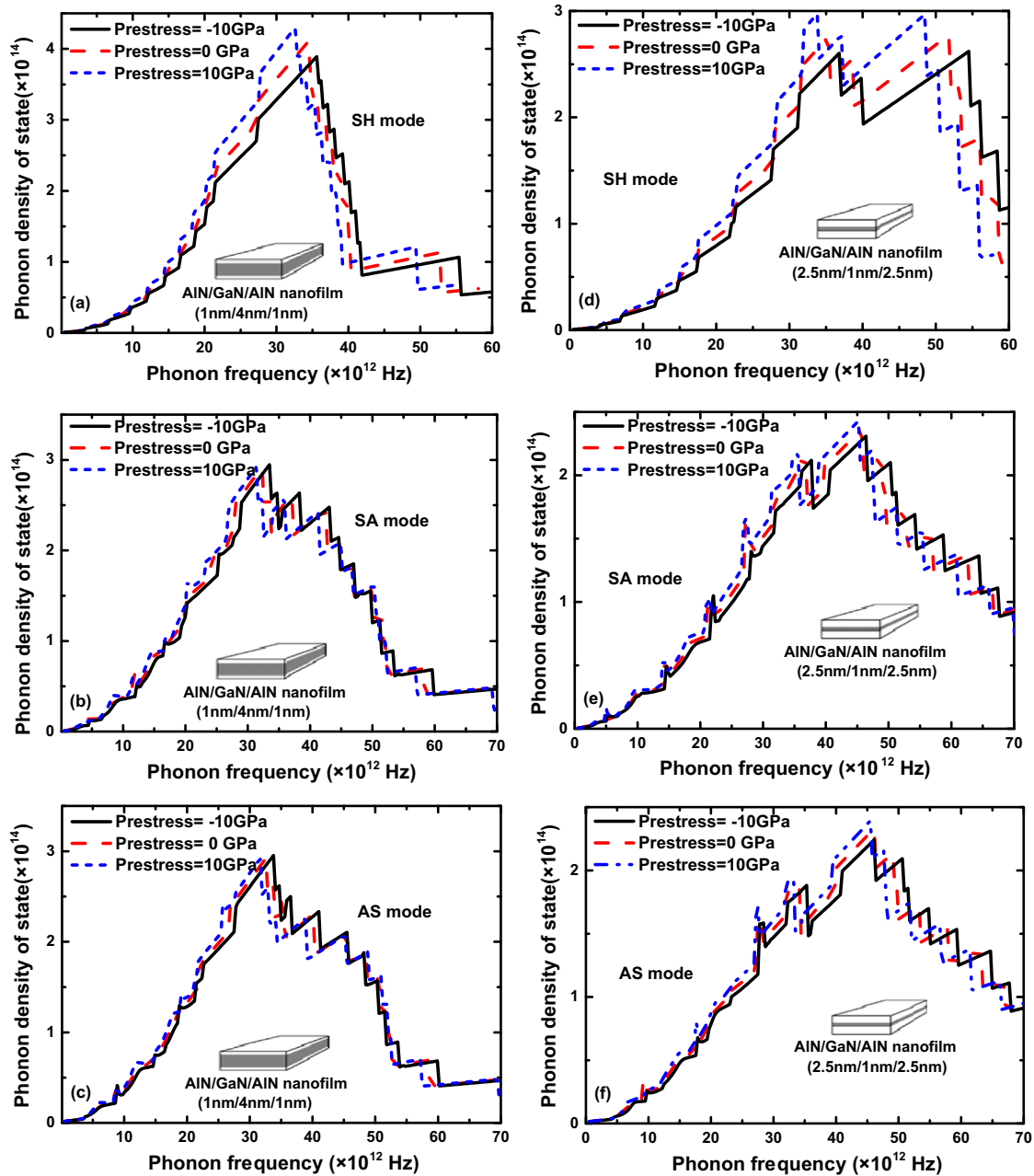
Fig. 7. Phonon density of states of the SH (a) (d), SA (b) (e), and AS (c) (f) modes for two heterostructures 1 nm/4nm/1 nm in (a), (b), and (c) as well as 2.5 nm/1nm/2.5 nm in (d), (e), and (f). The prestresses are −10 GPa, 0 GPa, 10 GPa.

and the phonon density of state for wurtzite GaN nanofilm, AlN nanofilm and the AlN/GaN/AlN nanofilm, respectively.

The phonon dispersion relations of SH, SA and AS modes for different types of nanofilms are firstly calculated, as shown in Fig. 1. Four types of nanofilms are pure AlN nanofilm and pure GaN nanofilms with 6 nm thickness, and AlN/GaN/AlN nanofilms with the thickness of 2.5 nm/1 nm/2.5 nm and 1 nm/5 nm/1 nm, respectively. According to the numerical results as plotted in Fig. 1 (a) and (g), the homogenous nanofilms in SH mode have phonon dispersion relations that stretch simply within a straight line, which is the dispersion relation of corresponding bulk structures. Due to the symmetrical property in AlN/GaN/AlN nanofilm, one can find from Fig. 1(c) and (e) that heterostructures have several curves overlapping each other. We also can notice that with increasing the thickness of GaN layer as shown in Fig. 1(a), (c),

(e) and (g), the phonon energy is decreases and the slops of curves becomes smaller. For the AS/SA modes, it can be noted that there are one inclination line for homogenous structures as shown in Fig. 1(b) and (h), and two inclination lines for heterostructures in Fig. 1(d) and (f). These inclination lines represent the corresponding phonon dispersion relations for bulk AlN and GaN. With the value of wave vector increased, the phonon energy approaches to these inclination lines. Similar to what we have found in the SH mode, the SA/AS modes have the lower energy with the thicker GaN layer when keeping the same thickness of nanofilms.

According to the definition of phonon group velocity, we can further calculate the phonon group velocities for SH, SA and AS modes based on the determined phonon dispersion relations. Fig. 2 depicts the phonon group velocities of SH mode and SA mode varied with the wave vector for four types of structures. One can

see from the figure that there are two straight lines, the one with larger value represents the group velocity of bulk AlN and the other is for bulk GaN. It can be clearly noticed that all the curves finally converge and gather together with the lines for bulk counterpart. For homogenous structures as shown in Fig. 2(a, b, g, h), the lines gradually approach to one value as the k increases. The heterostructures have two saturated values of convergences due to two different group velocities for bulk AlN and GaN, as shown in Fig. 2(c, d, e, f). The tendencies of convergence in SA modes are similar to those in SH modes in homogenous structures, and the processes perform the oscillation behaviors only in SA modes. When the structure turns into heterostructure, the group velocity for SH modes can also have the oscillation behaviors, and the variation of group velocity for SA modes become more complicated, seen in figures (d, f).

We further get the average group velocities of SH, SA, AS modes for different types of structures in Fig. 3. Due to the spatial confinement effects on the phonon dispersion relations, the average group velocities perform the oscillation behaviors with increasing the phonon energy in all structures. However, it can be found from the figure that the heterostructures display much more complicated oscillation behaviors than that for the homogenous structures. Moreover, clearly noted is that decreasing the thickness of AlN layer in the structures causes the peaks lower and the velocities smaller. Fig. 4 shows phonon density of states of SH, SA, AS modes for nanofilms with homogenous structures and heterostructures. One can notice that the peaks of DOS curves become higher and appear earlier when the thickness of GaN layer raises, and the variation of DOS for the SH modes is more significant than that for SA and AS modes.

After the discussion of heterogenicity effects on the phonon properties of nanofilms, we then apply the prestress field to identify its influence on phonon properties in heterostructural AlN/GaN/AlN nanofilms. Fig. 5(a and b) plots the phonon dispersion relations under the prestresses of -10 GPa, 0 GPa, and 10 GPa for SH mode as an example. One can notice that the phonon energy almost has no change for the small wave vector when the prestresses applied. With the increment of the wave vector, the effect of prestress fields becomes more and more significant. It also can be noted from Fig. 5(a and b) that the compressive stress enhances the phonon energy while the tensile stress reduces the energy, which is consistent with the MD simulations for stressed Si qualitatively [32]. With decreasing the thickness of GaN layer, the phonon energy is much more sensitive to the prestress fields. From the dispersion relations of SH modes in stressed heterostructural nanofilms, we can calculate the phonon group velocities of AlN/GaN/AlN nanofilms with 1 nm-4 nm-1 nm thickness and 2.5 nm-1 nm-2.5 nm thickness, as shown in Fig. 5(c and d). These two structures give similar variation trend that phonon group velocities become lower when higher prestresses are applied. However, the prestress performs the more significant influence when the thickness of GaN layer becomes thinner.

After suffering from prestress fields, the phonon average group velocities of AlN/GaN/AlN nanofilms can be further simulated for SH, SA and AS modes, as plotted in Fig. 6. We can observe that the prestress can modify the phonon average group velocities of SH mode remarkably, while the influence of prestress field on the phonon average group velocities is weaker for SA and AS modes. In most cases, the negative stress improves the velocity while the positive stress decreases the velocity. It is also noticeable that with decreasing the thickness of GaN layer, the velocities become greater for all modes and there is no significant difference for the change of velocities under prestress fields. Based on the definition of phonon density of state (DOS), we calculate the phonon DOS of AlN/GaN/AlN nanofilms under different prestresses, as shown in Fig. 7. One can find that the difference between DOS curves under various prestress in SA and AS modes are relatively weaker than that in SH modes. Similarly, decreasing the thickness of GaN layer could lead to the more significant influence of prestress fields on the DOS. Furthermore, it also can be noted that the positive stress increases the phonon DOS while the negative stress decreases the DOS.

5. Conclusion

To summary, the influences of the heterogenicity and prestress field on the phonon properties in semiconductor nanofilms were investigated theoretically. The continuum elastic model is utilized to describe the spatial confinement effect and acoustoelastic effect in semiconductor nanofilms. Numerical results demonstrated that the various heterostructures provide different phonon properties compared with the homogenous structures, and the prestress fields deliver significant impacts in phonon properties including phonon dispersion relation, phonon group velocity, phonon density of state, and phonon average group velocity. According to the phonon engineering, the heterogenicity and stress fields could be regarded as the alternative approaches to modify the phonon properties, so as to control the thermal and electrical properties in nanostructured semiconductors. Therefore, the present work could provide an efficient method for the thermal management in nanoelectronic devices.

References

[1] W. Sun, C.-K. Tan, N. Tansu, AlN/GaN digital alloy for mid- and deep-ultraviolet optoelectronics, Sci. Rep. 7 (2017) 11826.

[2] A.H. Park, T.H. Seo, S. Chandramohan, G.H. Lee, K.H. Min, S. Lee, M.J. Kim, Y.G. Hwang, E.-K. Suh, Efficient stress-relaxation in InGaN/GaN light-emitting diodes using carbon nanotubes, Nanoscale 7 (2015) 15099–15105.

[3] K. Lee, J.-W. Park, Y. Tchoe, J. Yoon, K. Chung, H. Yoon, S. Lee, C. Yoon, B.H. Park, G.-C. Yi, Flexible resistive random access memory devices by using NiOx/GaN microdisk arrays fabricated on graphene films, Nanotechnology 28 (2017) 205202.

[4] P. Bousoulas, J. Giannopoulos, K. Giannakopoulos, P. Dimitrakis, D. Tsoukalas, Memory programming of TiO2-x films by Conductive Atomic Force Microscopy evidencing filamentary resistive switching, Appl. Surf. Sci. 332 (2015) 55–61.

[5] R. Vitushinsky, M. Crego-Calama, S.H. Brongersma, P. Offermans, Enhanced detection of NO2 with recessed AlGaN/GaN open gate structures, Appl. Phys. Lett. 102 (2013) 172101.

[6] R. Chowdhury, F. Scarpa, S. Adhikari, Molecular-scale bio-sensing using armchair graphene, J. Appl. Phys. 112 (2012) 014905.

[7] A. Taube, J. Judek, C. Jastrzębski, A. Duzynska, K. Świtkowski, M. Zdrojek, Temperature-dependent nonlinear phonon shifts in a supported MoS2 monolayer, Appl. Mater. Interfaces 6 (2014) 8959–8963.

[8] Z.P. Xu, Heat transport in low-dimensional materials: a review andperspective, Theor. Appl. Mech. Lett. 6 (2016) 113–121.

[9] Y.H. Yu, Y.Y. Gao, J.Z. Song, Recent advances on thermal analysis of stretchable electronics, Theor. Appl. Mech. Lett. 6 (2016) 32–37.

[10] Z. Zabihi, H. Araghi, Effect of functional groups on thermal conductivity of graphene/paraffin nanocomposite, Phys. Lett. A 380 (2016) 3828–3831.

[11] Z. Zabihi, H. Araghi, Effective thermal conductivity of carbon nanostructure based polyethylene nanocomposite: Influence of defected, doped, and hybrid filler, Int. J. Therm. Sci. 120 (2017) 185–189.

[12] E.P. Pokatilov, D.L. Nika, A.A. Balandin, Acoustic-phonon propagation in rectangular semiconductor nanowires with elastically dissimilar barriers, Phys. Rev. B 72 (2005) 113311.

[13] A.A. Balandin, E.P. Pokatilov, D. Nika, Phonon engineering in hetero- and nanostructures, J. Nanoelectron. Optoelectron. 2 (2007) 140–170.

[14] Z. Tian, S. Lee, G. Chen, Heat transfer in thermoelectric materials and devices, ASME J. Heat Transfer 135 (2013) 061605.

[15] Y.Q. Jiang, S. Cai, Y. Tao, Z.Y. Wei, K.D. Bi, Y.F. Chen, Phonon transport properties of bulk and monolayer GaN from first-principles calculations, Compt. Mater. Sci. 138 (2017) 419–425.

[16] H. Bracht, S. Eon, R. Frieling, A. Plech, D. Issenmann, D. Wolf, J.L. Hansen, A.N. Larsen, J.W. Ager III, E.E. Haller, Thermal conductivity of isotopically controlled silicon nanostructures, New. J. Phys. 16 (2014) 015021.

[17] J. Groenen, C.M.S. Torres, M. Prunnila, J. Ahopelto, Inelastic light scattering by longitudinal acoustic phonons in thin silicon layers: From membranes to silicon-on-insulator structures, Phys. Rev. B 77 (2008) 045420.

[18] J. Zou, A.A. Balandin, Phonon heat conduction in a semiconductor nanowire, J. Appl. Phys. 89 (2001) 2932–2938.

[19] J.T.M. Beek, R. Puers, A review of MEMS oscillators for frequency reference and timing applications, J. Micromech. Microeng. 22 (2011) 1–35.

[20] L.L. Zhu, H.N. Luo, On the role of piezoelectricity in phonon properties and thermal conductivity of GaN nanofilms, Theor. Appl. Mech. Lett. 6 (2016) 277–281.

[21] L.M. Sandonas, G. Cuba-Supanta, R. Gutierrez, A. Dianat, C.V. Landauro, G. Cuniberti, Enhancement of thermal transport properties of asymmetric Graphene/hBN nanoribbon heterojunctions by substrate engineering, Carbon 124 (2017) 642–650.

[22] A. Soleimani, H. Araghi, Z. Zabihi, A. Alibakhshi, A comparative study of molecular dynamics simulation methods for evaluation of the thermal conductivity and phonon transport in Si nanowires, Compt. Mater. Sci 142 (2018) 346–354.

[23] M. Royo, M.D. Luca, R. Rurali, l. Zardo, A review on III–V core–multishell nanowires: growth, properties, and applications, J. Phys. D: Appl. Phys. 50 (2017) 143001.

[24] A. Ajay, C.B. Lim, D.A. Browne, J. Polaczyński, E. Bellet-Amalric, J. Bleuse, M.I. den Hertog, E. Monroy, Effect of doping on the inter-subband absorption in Si- and Ge-doped GaN/AlN heterostructures, Nanotechnology 28 (2017) 405204.

[25] X.Y. Zhang, W. Liu, J. Zhou, D.H. Yue, J. Wang, C. Liu, Y. Huang, Y. Liu, Y.H. Zhou, A direct tensile device to investigate the critical current properties in superconducting tapes, Rev. Sci. Instrum. 85 (2014) 025103.

[26] H.D. Yong, M. Zhao, Z. Jing, Y.H. Zhou, Effect of shear stress on electromagnetic behaviors in superconductor-ferromagnetic bilayer structure, J. Appl. Phys. 116 (2014) 123911.

[27] L.L. Zhu, Electron-acoustic phonon interaction and mobility in stressed rectangular silicon nanowires, Chin. Phys. B 24 (2015) 016201.

[28] Y. Hou, L.L. Zhu, Influence of surface scattering on the thermal properties of spatially confined GaN nanofilm, Chin. Phys. B 25 (2016) 086502.

[29] J.J. Cao, X.F. Gou, Pressure effect on the mechanical, electronic and thermodynamic properties of Ba2Bi3: First-principle calculations, J. Phys. Chem. Solids 104 (2017) 293–303.

[30] J.B. Wen, J.J. Zhang, Y.W. Gao, A coupling finite element model for analysis the nonlinear dynamic magnetoelectric response of tri-layer laminate composites, Comp. Struct. 166 (2017) 163–176.

[31] H.N. Luo, L.L. Zhu, Effects of surface stress on the phonon properties in GaN nanofilms, J. Appl. Mech. 82 (2015) 111002.

[32] X. Li, K. Maute, M.L. Dunn, R. Yang, Strain effects on the thermal conductivity of nanostructures, Phys. Rev. B 81 (2010) 245318.

[33] L.L. Zhu, H.N. Luo, Phonon properties and thermal conductivity of GaN nanofilm under prestress and surface/interface stress, J. Alloy. Comp. 685 (2016) 619–625.

[34] A. Shchepetov, M. Prunnila, F. Alzina, L. Schneider, J. Cuffe, H. Jiang, E.I. Kauppinen, C.M. Sotomayor Torres, J. Ahopelto, Ultra-thin free-standing single crystalline silicon membranes with strain control, Appl. Phys. Lett. 102 (2013) 192108.

[35] A. Balandin, K.L. Wang, Significant decrease of the lattice thermal conductivity due to phonon confinement in a free-standing semiconductor quantum well, Phys. Rev. B 58 (1998) 1544.

[36] Y.-H. Pao, U. Gamer, Acoustoelastic waves in orthotropic media, J. Acoust. Soc. Am. 77 (1985) 806–812.

[37] L.L. Zhu, X.J. Zheng, Modification of the phonon thermal conductivity in spatially confined semiconductor nanofilms under stress fields, EPL 88 (2009) 36003.

[38] R. Abramson, C.L. Tien, A. Majumdar, Interface and strain effects on the thermal conductivity of heterostructures: a molecular dynamics study, J. Heat Transfer 124 (2002) 963–970.

[39] A.R. Bhatt, K.W. Kim, M.A. Stroscio, J.M. Higman, Simplified microscopic model for electron-optical-phonon interactions in Quantum wells, Phys. Rev. B 48 (1993) 14671–14674.

[40] N. Bannov, V. Aristov, V. Mitin, M.A. Stroscio, Electron relaxation times due to the deformation-potential interaction of electrons with confined acoustic phonons in a free-standing quantum well, Phys. Rev. B 51 (1995) 9930–9942.

[41] A.V. Osetrov, H.-J. Fröhlich, R. Koch, E. Chilla, Acoustoelastic effect in anisotropic layered structures, Phys. Rev. B 62 (2000) 13963.

[42] J. Zou, X. Lange, C. Richardson, Lattice thermal conductivity of nanoscale AlN/GaN/AlN heterostructures: effects of partial phonon spatial confinement, J. Appl. Phys. 100 (2006) 104309.

[43] L.L. Zhu, H.H. Ruan, Influence of prestress fields on the phonon thermal conductivity of GaN nanostructures, ASME J. Heat Transfer 136 (2014) 102402.

[44] L.L. Zhu, H.H. Ruan, Effects of pre-stress and surface stress on phonon thermal conductivity of rectangular Si nanowires, Appl. Phys. A 119 (2015) 253–263.

[45] M. Łopuszyński, J.A. Majewski, Ab initio calculations of third-order elastic constants and related properties for selected semiconductors, Phys. Rev. B 76 (2007) 045202.